Available online at www.sciencedirect.com
ScienceDirect
Journal of Sound and Vibration 311 (2008) 707–728
JOURNAL OF SOUND AND VIBRATION
www.elsevier.com/locate/jsvi

Multiharmonic excitation for nonlinear system identification

M.D. Narayanan, S. Narayanan, Chandramouli Padmanabhan*

Machine Design Section, Department of Mechanical Engineering, Indian Institute of Technology Madras, Chennai 600 036, India

Received 23 March 2006; received in revised form 15 June 2007; accepted 23 September 2007
Available online 26 October 2007

Abstract

Parametric identification of nonlinear systems is done using a hybrid time/frequency-domain-based Fourier series identification method. A multiharmonic force excitation is proposed to overcome identification problems encountered with a single harmonic excitation for certain classes of nonlinear systems. A Duffing oscillator and a system with quadratic damping are considered in detail for illustration of the proposed identification scheme using multiharmonic excitation. It is demonstrated that for most situations a multiharmonic excitation leads to significantly better identification results than a single harmonic excitation-based method.

1. Introduction

In many applications, the systems are nonlinear or the effect of nonlinearity cannot be ignored. In such cases, nonlinear system identification has to be carried out. The presence of nonlinearities poses challenges. There are wide varieties of methods available for nonlinear system identification. If the mathematical structure of the governing equations of the system is assumed or known a priori, the problem of identification reduces to the determination of unknown physical parameters of the system. This problem is termed as parametric identification. If the structure of equations is also unknown, the problem is called non-parametric identification. In the present work, the area of investigation is confined to the parametric identification of systems subjected to periodic excitation and having a periodic response.

Worden and Tomlinson [1] gave an overview of the broad category of methods in modal analysis applied to nonlinear systems. In one of the early classical papers on nonlinear system identification, Masri and Caughey [2] used the state variables of nonlinear systems to express the system characteristics in terms of orthogonal functions. Crawley and Aubert [3] used the technique of force–state mapping to obtain the nonlinearities in the joints of space structure. Mohammad et al. [4] suggested a method for directly estimating the physical parameter matrices of the linear and nonlinear structures. The work takes into account a variety of nonlinearities of arbitrary order. Perona et al. [5] used a trajectory method for reconstruction of ordinary differential equations from a given time-series trajectory. Some form of the method of least squares is used in these papers where the system excitation and response need not be periodic.

*Corresponding author. Tel.: +91 44 22574690; fax: +91 44 22574652.
E-mail address: mouli@iitm.ac.in (C. Padmanabhan).

0022-460X/$ - see front matter © 2007 Elsevier Ltd. All rights reserved.
doi:10.1016/j.jsv.2007.09.019

There are identification techniques based on the periodicity of the excitation and response. Yasuda et al. [6] applied the harmonic balance method (HBM) for identification of nonlinear multidegree-of-freedom (mdof) systems. They approximated the nonlinearity in the system using polynomials and the response of the system was represented by a truncated Fourier series. Yuan and Feeny [7] used the technique of combining the periodic orbit extraction and harmonic balance scheme for the parametric identification of chaotic systems. Thothadri et al. [8] used the principle of HBM to identify mdof systems. They used a methodology called harmonic balance nonlinearity identification, which helps to identify parameters in self-excited motions of a fluid structure system. The method uses higher order harmonics contained in the data to recover the nonlinearities required to model the dynamics. Doughty et al. [9] have presented a comparative study of the parameter estimation of a cantilever beam, subjected to a base excitation, and assumed to be transversely vibrating in a single mode. Three techniques have been compared, with the first method based on continuous time differential equation, the second on HBM and the third on method of multiple scales.

In using HBM for system identification, numerical difficulties arise, which has not been highlighted by the above-mentioned investigations. This is related to the pseudo-inversion of the ill-conditioned matrix corresponding to the set of linear equations obtained by the process of approximating the solution by a Fourier series. Another problem is that even if the inversion of the matrix is proper, the identified values may not be correct. This is because even though the forward problem may yield unique solutions, the corresponding algebraic inverse form is unique only in the least squares sense. Thus, it is seen that the accuracy of identification depends on the structure of the generated data set, which in turn depends on the excitation. Thus, the successful identification depends on the choice of a suitable excitation signal.

Most of the investigations, using HBM, have been confined to a sinusoidal excitation and guidelines on the choice of excitation amplitude and frequency have not been adequately discussed. The main objective of this paper is to develop a robust identification procedure using a hybrid frequency/time-domain version of HBM. While a number of different parametric identification methods are available, the harmonic/periodic excitation-based identification method has been chosen, since this is the form of excitation that exists in a number of practical mechanical systems. In this work, an inverse form of the Fourier series method, denoted as Fourier series identification method (FSIM), is used for system identification. This method is quite similar to the conventional HBM; the difference between HBM and FSIM is summarized in Fig. 1. There are two stages in the identification denoted by two blocks 1 and 2 for HBM, 1 and 3 for FSIM. In HBM, both the stages are

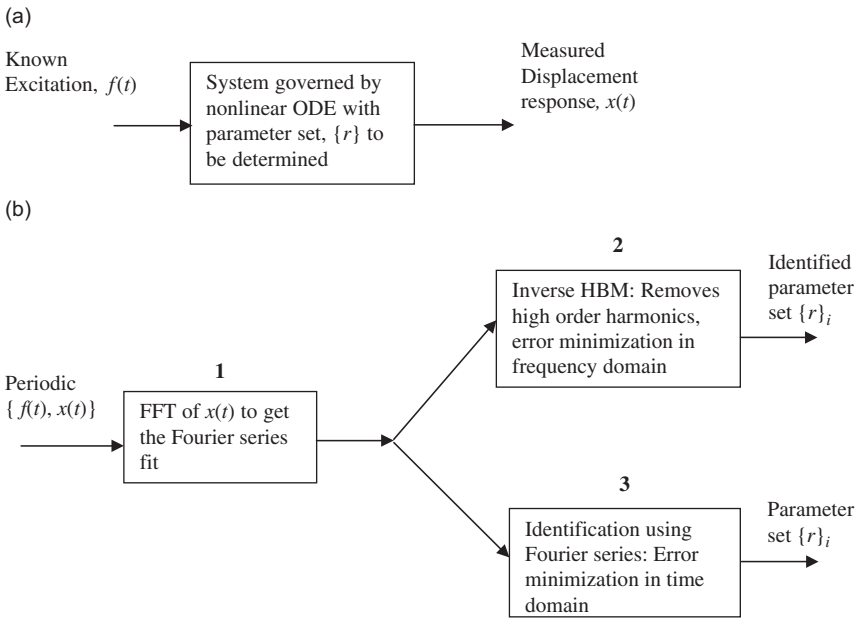

Fig. 1. (a). The identification problem and (b). The identification scheme and terminology. Items 1 and 2 together is termed as identification by HBM. Items 1 and 3 together are termed as FSIM.

done in the frequency domain whereas in FSIM the first stage is in the frequency domain and the second stage is the time domain. The condition under which these two schemes yield the same results is established in Appendix A. In this process, a correction is suggested in the original formulation of HBM as used by other investigators.

In the present work, the excitation is assumed to be harmonic/periodic and the response of the system is assumed to be periodic. Though the scheme of FSIM is easy in implementation, there may be considerable error in the parameter estimates if a single harmonic excitation is used as shown later in the paper. In order to improve the success in the identification a multiharmonic excitation is proposed.

The following natural questions arise on the choice of the excitation signal for system identification: (i) What combination of amplitude and frequency of the harmonic excitation will yield good identification results? (ii) A broader question is, are there better candidates for the input signal? A multiharmonic force excitation with suitably chosen amplitudes and frequencies is proposed as a solution to the second question. However, the choice of the excitation parameters in these cases is a difficult problem as there are numerous combinations of them. In this paper, an attempt is made to answer the above questions through computational experiments. A preliminary work of the present kind was carried out by authors [10]. A method of improving the identification based on a multiharmonic excitation is suggested. It is shown that for a Duffing oscillator and a system with quadratic damping, multiharmonic excitation improves the identification results significantly for a broad range of excitation frequencies and amplitudes. A mdof system is also considered to establish the improvement with multiharmonic excitation.

2. Fourier series identification method

A review of the parametric identification using FSIM is given in this section. Vibratory systems governed by nonlinear ordinary differential equations and subjected to harmonic/periodic force excitations are considered. Further, it is assumed that the response of the system is periodic. It is assumed that the simulation/experimental data of the excitation force $f(t)$ and the displacement response $x(t)$ over a steady-state period is available for analysis. The advantage of FSIM or HBM compared with techniques having non-periodic response is that, since the response is periodic, given $x(t)$, the velocity $v(t)$ and acceleration $a(t)$ are obtainable by direct differentiation rather than numerical differentiation. Instead of $x(t)$, if $a(t)$ is available, $v(t)$ and $x(t)$ can be obtained by direct integration. In this work, $x(t)$ is chosen as it can then include the 'mean response'. If $a(t)$ is chosen instead one has difficulty in determining the mean response while integrating. In the FSIM, the periodic response of the system is expressed in terms of a truncated Fourier series with terms having frequencies, which are integer multiples/sub-multiples of the excitation frequency. The coefficients of the harmonic terms are obtained such that the resulting time series matches with the original one to the required degree of accuracy. The original response of the system in general cannot be represented in an analytical form, as the system is nonlinear. The Fourier series solution thus obtained can be used for system analysis as well as system identification.

In the identification scheme, the Fourier solution is substituted into the governing equation of motion, which gives an algebraic equation in terms of system parameters. Imposing the condition that this equation should be satisfied at all sample points in the time domain, yields a system of linear algebraic equations. This is solved using a pseudo-inversion technique to obtain the unknown system parameters.

2.1. Identification using FSIM

To illustrate the procedure, the harmonically forced Duffing oscillator is considered:

$$m\ddot{x} + c\dot{x} + kx + \alpha x^3 = f(t) = F\cos\Omega t, \tag{1}$$

where m, c, k and α are the mass, damping coefficient, linear stiffness and coefficient of the nonlinear term, respectively. They are the parameters of the system to be determined from the known input-response data. For the purpose of parametric identification, the oscillator is assumed to be excited with known harmonic excitation parameters, F and Ω. Assume that the response $x(t)$ of the vibrating system is known and is periodic with a fundamental period $T = 2\pi/\Omega$. Expressing the response in a truncated M term harmonic Fourier series

one has

$$x(t) = a_0 + \sum_{j=1}^{M}(a_j \cos j\Omega t + b_j \sin j\Omega t). \tag{2}$$

Substituting this periodic solution in Eq. (1), one obtains

$$\begin{aligned} &- m\sum_{j=1}^{M}(a_j j^2\Omega^2 \cos j\Omega t + b_j j^2\Omega^2 \ \sin \ j\Omega t) + c\sum_{j=1}^{M}(-a_j j\Omega \ \sin \ j\Omega t + b_j j\Omega \ \cos \ j\Omega t) \\ &+ k(a_0 + \sum_{j=1}^{M}(a_j \ \cos \ j\Omega t + b_j \ \sin \ j\Omega t)) + \alpha(a_0 + \sum_{j=1}^{M}(a_j \cos j\Omega t + b_j \ \sin \ j\Omega t))^3 = F \cos \Omega t. \end{aligned} \tag{3}$$

Eq. (3) can be written compactly as

$$mp_1(t) + cp_2(t) + kp_3(t) + \alpha p_4(t) = p_5(t), \tag{4}$$

where

$$\begin{aligned} &p_1(t) = \ -\Omega^2\sum_{j=1}^{M} j^2(a_j \cos j\Omega t + b_j \sin j\Omega t); \quad p_2(t) = \Omega\sum_{j=1}^{M} j(-a_j \sin j\Omega t + b_j \cos j\Omega t), \\ &p_3(t) = a_0 + \sum_{j=1}^{M}(a_j \cos j\Omega t + b_j \sin j\Omega t); \quad p_4(t) = (a_0 + \sum_{j=1}^{M}(a_j \cos j\Omega t + b_j \sin j\Omega t))^3, \\ &p_5(t) = F \ \cos \ \Omega t. \end{aligned} \tag{5}$$

For a set of N discrete, equally spaced time samples in one excitation time period T the matrix form of the above equation becomes

$$\begin{bmatrix} p_1(0) & p_2(0) & p_3(0) & p_4(0) \\ p_1(\Delta t) & p_2(\Delta T) & p_3(\Delta T) & p_4(\Delta T) \\ \vdots & \vdots & \vdots & \vdots \\ p_1((N-1)\Delta t) & p_2((N-1)\Delta t) & p_3((N-1)\Delta t) & p_4((N-1)\Delta t) \end{bmatrix} \begin{Bmatrix} m \\ c \\ k \\ \alpha \end{Bmatrix} = \begin{Bmatrix} p_5(0) \\ p_5(\Delta t) \\ \vdots \\ p_5((N-1)\Delta t) \end{Bmatrix}. \tag{6}$$

Eq. (6) can be written compactly as

$$[G]\{r\} = \{f\}, \tag{7}$$

where $\{r\} = [m \ c \ k \ \alpha]^{\mathrm{T}}$ is the parameter set, where superscript T indicates transpose. The identified parameter set $\{r\}_i$ is obtained as

$$\{r\}_i = [G]^{+}\{f\} = [D]^{-1}[G]^{\mathrm{T}}\{f\}, \tag{8}$$

where $[G]^{+}$ is the pseudo-inverse of $[G]$ and

$$[D] = [G]^{\mathrm{T}}[G] = \begin{bmatrix} p_1(0) & \cdots & p_1((N-1)\Delta t) \\ p_2(0) & \cdots & p_2((N-1)\Delta t) \\ p_3(0) & \cdots & p_3((N-1)\Delta t) \\ p_4(0) & \cdots & p_4((N-1)\Delta t) \end{bmatrix}$$

$$\times \begin{bmatrix} p_1(0) & p_2(0) & p_3(0) & p_4(0) \\ \vdots & \vdots & \vdots & \vdots \\ p_1((N-1)\Delta t) & p_2((N-1)\Delta t) & p_3((N-1)\Delta t) & p_4((N-1)\Delta t) \end{bmatrix}$$

$$= \begin{bmatrix} \sum_{i=0}^{N-1} (p_1(i\Delta t))^2 & \sum p_1(i\Delta t)p_2(i\Delta t) & \sum p_1(i\Delta t)p_3(i\Delta t) & \sum p_1(i\Delta t)p_4(i\Delta t) \\ \cdot & \sum (p_2(i\Delta t))^2 & \sum p_2(i\Delta t)p_3(i\Delta t) & \sum p_2(i\Delta t)p_4(i\Delta t) \\ \cdot & \cdot & \sum (p_3(i\Delta t))^2 & \sum p_3(i\Delta t)p_4(i\Delta t) \\ \cdot & \cdot & \cdot & \sum (p_4(i\Delta t))^2 \end{bmatrix}. \quad (9)$$

The pseudo-inverse is equivalent to the least squares minimization of $||[G]\{r\} - \{f\}||_2$. The above formulation can be applied to other types of systems having smooth nonlinearities. Invertibility of the $[D]$ matrix plays a crucial role in successful identification. While it is clear that the excitation parameters will influence the relative values of the elements of the $[D]$ matrix, the appropriate choice of these parameters a priori is difficult.

As seen from Appendix A, one could use either the hybrid frequency/time-domain-based method described above or a frequency-domain method; these are equivalent. The time-domain method is advantageous since the nonlinearities are easier to calculate in the time domain. The issue of how many terms to be retained in the HBM for convergence does not arise in the FSIM case and hence for the rest of the paper this technique is used.

2.2. Direct determination of error in parameters

If the identification is carried out using the simulated data as mentioned earlier, the parameters of the original and the identified system are available for error estimation. Error measures based on difference in parameter values for a Duffing oscillator can be defined as

$$m_e = (m - m_i)/m; c_e = (c - c_i)/c; k_e = (k - k_i)/k; \alpha_e = (\alpha - \alpha_i)/\alpha, \quad (10)$$

where subscript i represents the identified parameters and m_e, c_e, k_e and α_e are the normalized errors in the identification of mass, damping, linear stiffness and nonlinear stiffness, respectively. The total parameter error E_p is computed as

$$E_p = \sqrt{(m_e^2 + c_e^2 + k_e^2 + \alpha_e^2)/n_p}, \quad (11)$$

where n_p is the number of parameters, equal to four in this case. One of the most commonly used error norm in identification is root mean square (rms) error in the response defined as

$$E_r = \sqrt{\frac{1}{T}\int_{t=0}^{T} [x_i(t) - x(t)]^2 \, \mathrm{d}t}, \quad (12)$$

where $x_i(t)$ is the response based on the identified parameters. This error will not enable us to judge the robustness of the algorithm. First, the pseudo-inverse used in the identification will lead to a least square error minimization of the algebraic sum of the forces in the governing equation. Based on the studies done (see Appendix A for details) it is clear that E_r is not well correlated with E_p in many situations. i.e. a minimum of E_r does not necessarily imply a minimum of E_p and vice versa. In an experimental scenario, only a measurable norm like E_r is available for checking the correctness of the result. However, in the development of this algorithm, E_p as defined in this paper can be estimated since the study is done with known input, output, as well as system parameters. This can be used to check the quality of the identification algorithm itself. There is another reason for using the parametric norm, since there are investigations with single and multiharmonic

excitations and it will not make sense to compare E_r in these two cases, as the response trajectories are different for both cases.

2.3. Implementation

If the periodic response of a system is given, an approximate solution for the system can be accomplished by performing a discrete Fourier transform (DFT) on the response data. The data points are usually equally spaced in time. In practice, a fast Fourier transform (FFT) is used. The FFT coefficients, which are complex, may be converted into equivalent real-valued Fourier series coefficients. Following this, the system identification by pseudo-inverse as mentioned above can be done.

Parametric identification of the Duffing oscillator illustrated in the previous section is carried out using the FSIM. To generate data for the study, the periodic response of a known system to a harmonic excitation is obtained by numerical integration in MATLAB. The above data is transformed to the frequency domain, to obtain the Fourier series solution to the problem. Using the above input–output data again, the FSIM is made use of to identify the parameters of the system. The number of sampling points N considered in this case is 128. N is chosen to ensure that the frequency range of interest is covered. The equally spaced sampling time interval is $\Delta t = T/N$ where T is the steady-state period of response. Relatively insignificant Fourier coefficient terms are not included in the analysis. This is done by specifying a tolerance for the rms for the terms truncated in the Fourier series. The following tolerance criterion is used for the truncation of the Fourier series coefficients, with $a_{\text{rms}}^{\text{trunc}}$ representing the rms value of the truncated terms, a_{rms} representing the total rms value of the response signal and ε the specified tolerance:

$$a_{\text{rms}}^{\text{trunc}}/a_{\text{rms}} < \varepsilon. \tag{13}$$

In this study, the tolerance ε is chosen as 10^{-6}. This tolerance is used to filter out higher order harmonic terms if any, which are extremely small in values. The identification result is not affected by this truncation, but the number of terms in the series is reduced considerably, thereby saving computational effort involving terms with nearly zero values. The result obtained for a case with single harmonic excitation is shown in Table 1 and Fig. 2. The original time series of response and the response generated from the identified parameters are plotted together.

3. Identification: single harmonic vs. multiharmonic excitation

In this section, a single, two and three harmonic inputs, denoted as 1-H, 2-H and 3-H, respectively, are considered for the identification. A comparative study between these excitations on the success of identification is carried out. The excitation mean load is taken as zero. Consider a Duffing oscillator subjected to the excitation

$$m\ddot{x} + c\dot{x} + kx + \alpha x^3 = \sum_{j=1}^{L} F_{Lj}\cos(j\Omega t + \phi_j), \tag{14}$$

where $L = 1$, 2 or 3. The higher frequencies are integer multiple of the fundamental frequency Ω. The phase angles $\{\phi_j\}$ are taken as 0, $\{0, \pi\}$ and $\{0, 2\pi/3, 4\pi/3\}$ for $L = 1$, 2 and 3, respectively. In order to compare the performance of three cases, the rms values of the excitations in Eq. (14) are adjusted to be equal by the

Table 1
Nonlinear system identification using FSIM

Excitation: $F\cos(\Omega t)$; excitation parameters: $F = 3$, frequency ratio $\eta = \Omega/\omega_n = 0.4$
ω_n = undamped natural frequency of the corresponding linear system
Actual system parameters: $(r)^{\text{T}} = [m,c,k,\alpha] = [1.0,0.02,1,0.2]$
Corresponding identified parameters: $\{r\}_i^{\text{T}} = [m_i, c_i, k_i, \alpha_i] = [1.0002,0.0198,0.9996,0.2001]$
$E_r = 6.4719 \times 10^{-7}$, $E_p = 0.0061$

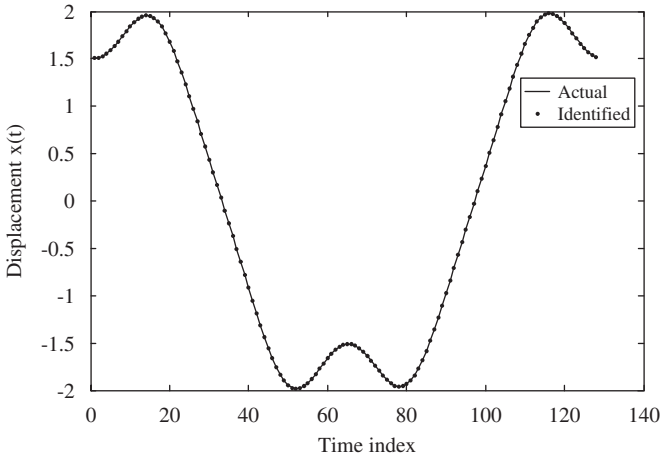

Fig. 2. Time series plot of the actual and the identified system. Solid line is the one-period steady-state response of the actual system. The dot symbols stands for the corresponding identified system.

Table 2
Forced excitation parameters: F_{Lj} is as given by Eq. (15)

1-H input	$F\cos(\Omega t)$
2-H input	$F_{21}\cos(\Omega t)+F_{22}\cos(2\Omega t+\pi)$
3-H input	$F_{31}\cos(\Omega t)+F_{32}\cos(2\Omega t+2\pi/3)+\ F_{33}\cos(3\Omega t+4\pi/3)$

following rule where the amplitude of excitation for 1-H excitation F_{11}, is denoted as F. Define

$$F_{\mathrm{Lj}} = \lambda_L F/j, \quad j = 1, 2, \ldots, L, \tag{15}$$

where L is the number of excitation harmonics, F_{Lj} is the amplitude of the jth harmonic term and λ_L is a coefficient determined using equal rms criterion, $F^2 = \Sigma_{j=1}^{L}(F_{Lj})^2$. Thus, for $L = 2$, $\lambda_L = \sqrt{4/5}$ and for $L = 3$, $\lambda_L = 6/7$. Table 2 gives the amplitudes and phases for $L = 1$, 2 and 3. The higher frequencies in the excitation were chosen to be integer multiples of the lowest frequency. This helps to simplify the response spectrum which in this case, generally consists of terms having frequencies which are integer multiples of the lowest frequency of excitation. Subharmonic response can also be dealt with this procedure; however, that is not considered here. If the multiple harmonics in the excitation are not chosen as above, combination tones of all orders can occur in the response and specialized multitone HB algorithms [11,12], will be required to obtain a representation of the steady-state response. The corresponding choice of the sampling rate is not trivial and it will amount to creating unnecessary complications in the identification procedure.

Since the work involves a comparative study there are a wide variety of choices available such as (i) number of harmonics in the excitation, (ii) the relative values of the amplitudes and phases of the harmonic terms in the excitation and (iii) the range of the excitation parameters. Thus, there are an unlimited number of choices for the type of multiharmonic excitation and certain criteria for the choice have to be fixed. The choice possible include, uniform amplitude, decreasing amplitude with different rate of decrease like exponentially decreasing, linearly decreasing, etc. and even increasing or mixed type (non-monotonic) amplitudes. In all these cases, the equality of total rms can be made to satisfy. The choice in the paper was made keeping in mind the applicability of the excitation signal. This has to be generated from a real system, which is physically sustainable. Decreasing amplitude for higher frequencies was chosen with these notions. Otherwise, the choice is arbitrary.

The parameters used in the simulation are given in Table 3. Three identification tests are conducted and the results are shown in the same table. The force amplitudes and phases are chosen as given in Table 2. The result

Table 3
Comparison of 1-H, 2-H and 3-H excitation for one set of data

$F=0.1$, $\eta=0.3$; $\{r\}^{T}=[1\ 0.02\ 1\ 0.2]$; mean square value of excitation $=0.005$; $\varepsilon=10^{-6}$							
Excitation harmonics	Excitation force amplitude/s	Identified parameters				E_p	l_c
		M	c	K	α		
1	0.1	0.7717	0.0199	0.9780	0.3613	0.4193	18.8324
2	[0.0894 0.0447]	0.9996	0.0200	1.0003	0.1762	0.0595	9.4201
3	[0.0853 0.0426 0.0284]	1.0010	0.0200	1.0040	0.1208	0.1980	7.8571

Table 4
Comparison of 1-H, 2-H and 3-H excitations over a range of excitation

Actual parameter set, $\{r\}^{T}=[1,0.02,1,0.2]$ Force range for F, $F_{min}=0.1$, $F_{max}=2$; frequency ratio range for η, $\eta_{min}=0.1$, $\eta_{max}=0.5$ Number of trials, $n=100$ (10×10) N_S: number of cases with $E_p\leqslant5\%$	% Success $=(N_S/n)\times100$
	% Success
1-H input	71.56
2-H input	94.67
3-H input	89.33

	Average of l_c
1-H input	9.4153
2-H input	4.9838
3-H input	5.1071

shows that two harmonic excitations give a much better result compared with one harmonic excitation. To examine the possible reason for improvement, consider the $[D]$ matrix in Eq. (9). The condition number of this matrix is evaluated for the three cases. The condition number is the ratio of the largest eigenvalue to the smallest eigenvalue of a matrix and it indicates the quality of inversion of the matrix. The logarithm of the condition number of the $[D]$ matrix is denoted as l_c and is given in the table. The result shows that there is a drastic drop in the condition number from 1-H to 2-H excitation. However, though there is reduction in l_c from 2-H to 3-H, the corresponding E_p is higher for 3-H. Most of the results in this paper is found to be qualitatively similar to the above result.

3.1. Comparison studies over the excitation parameter ($F-\eta$) space

A computational test to illustrate the improvement of results for 2-H and 3-H inputs over a 1-H input is given here. For comparison of these three excitations, the amplitudes and phases of excitations are chosen as given in Table 2. Identification tests were conducted for a set of parameters and a comparison for the success was made between 1-H, 2-H and 3-H excitations. Note that success is defined as those parameter sets for which $E_p\leqslant0.05$. The steady-state responses, which are not period-one (P-1), are excluded from the analysis; P-1 response has a fundamental period equal to the period of excitation. Table 4 and Fig. 3 show the comparisons for tests conducted over a range of excitation parameters. There is a significant improvement in the success of identification while employing a two-harmonic excitation in place of a single harmonic excitation. The performance of the three harmonic excitation lies in between the other two. One of the reasons for the reduction in success may be due to the excitation of the super-harmonic resonance when the third harmonic is used, as the nonlinearity is of the cubic type. The excitation frequencies are set below the resonant region. This was based on a preliminary study that yielded relatively poor results for the excitation near resonance. The reason for the poor results in the resonant region is that more of linear dependency is created in the data set between the displacement and the acceleration terms and hence in the corresponding columns of the $[G]$ matrix.

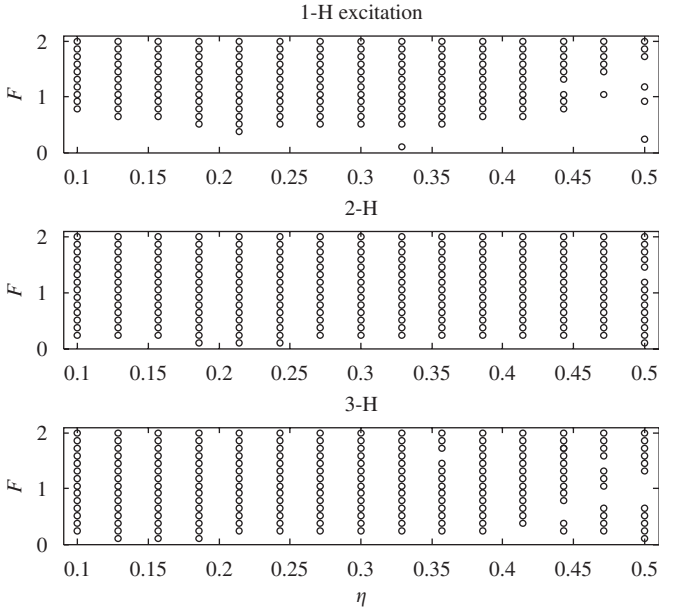

Fig. 3. Duffing oscillator: success over the excitation parameter space $F-\eta$ for 1-H, 2-H and 3-H cases. Symbol '○' stands for $E_p \leqslant 0.05$. The blank spaces correspond to either $E_p > 0.05$ or the response being non-P1 type.

4. Identification results using multiharmonic force excitation for different parameter sets

The identification tests are now carried out for a range of system parameter values. The results for a sdof Duffing oscillator and a system with quadratic damping are given. The system and the excitation parameter values are given in Table 5.

4.1. Duffing oscillator

Fig. 4 shows the comparison plots for three cases for a range of the parameter α. The two harmonic input case shows improvement in the identification results over the other two. Fig. 5 gives average value of l_c for three cases. There is a large drop in l_c from 1-H to 2-H/3-H. It may be concluded that changing from 1-H to multiharmonic excitation statistically gives better success and there is a corresponding lowering of condition number. When α is large the single harmonic case is reasonably good as the cubic term starts to dominate the response. Similar studies are conducted by varying the damping and the linear stiffness and the results are shown in Figs. 6 and 7. The linear stiffness causes poorer identification results as the nonlinear contribution to the response reduces.

The results similar to that given in Figs. 3 and 4 can be produced by a random generation procedure, which is given in Section 5. This helps to present and interpret results in an alternate way.

4.2. System with quadratic damping nonlinearity

Consider the equation with a quadratic damping nonlinearity given by

$$m\ddot{x} + c|\dot{x}|\dot{x} + kx = f(t). \tag{16}$$

The parameters to be identified are m, c and k. The identification scheme and the parametric error used are similar to that described in Section 2. Figs. 8–10 show the results. In these cases, the 2-H and 3-H inputs give nearly same results, which are much better than 1-H excitation.

Table 5
Multi-harmonic excitation: parameter setting for simulation

1. Duffing oscillator
(i) Parameter varied: nonlinear parameter α from 0.1 to 1. Mass, $m = 1$, damping, $c = 0.02$, linear stiffness, $k = 1$. excitation parameter (*EP*) range: force range, $F_{\min} = 0.1$, $F_{\max} = 2$; frequency ratio range, $\eta_{\min} = 0.1$, $\eta_{\max} = 0.5$
(ii) Parameter varied: c, $c_{\min} = 0.01$, $c_{\max} = 0.05$; $m = 1$; $k = 1$, $\alpha = 0.2$ *EP* range: $F_{\min} = 0.1$, $F_{\max} = 2.1$; $\eta_{\min} = 0.1$, $\eta_{\max} = 0.5$
(iii) Parameter varied: k, $k_{\min} = 0.1$; $k_{\max} = 2$; $m = 1$; $c = 0.02$; $\alpha = 0.2$; *EP* range: $F_{\min} = 0.5$; $F_{\max} = 2.1$; $\eta_{\min} = 0.1$, $\eta_{\max} = 0.4$

2. Quadratic damping nonlinearity
(i) Parameter varied—damping c, $c_{\min} = 0.01$, $c_{\max} = 0.05$, Mass $m = 1$; linear stiffness $k = 0.1$; EP range: $F_{\min} = 0.01$, $F_{\max} = 0.1$; $\eta_{\min} = 0.1$, $\eta_{\max} = 1$
(ii) Parameter varied—k, $k_{\min} = 0.1$, $k_{\max} = 2$; $m = 1$; $c = 0.02$; *EP* range: $F_{\min} = 0.5$, $F_{\max} = 2$; $\eta_{\min} = 0.1$, $\eta_{\max} = 1$

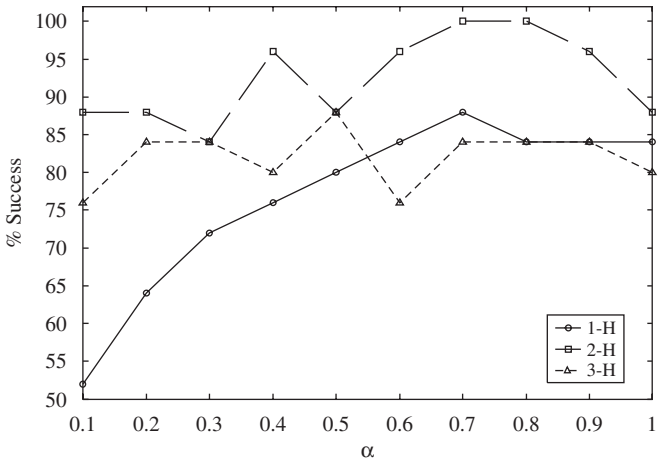

Fig. 4. Duffing oscillator: percentage success (for $E_p \leqslant 0.05$) variation with nonlinear parameter α. Twenty-five equally spaced points over $F-\eta$ grid, specified in Table 6, is used at each value of α to obtain this comparison.

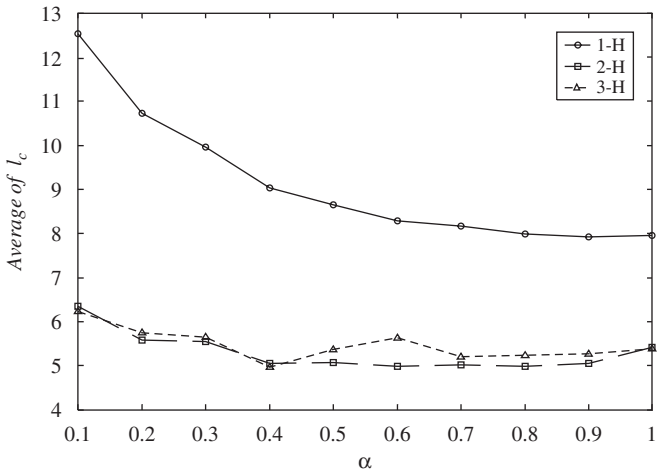

Fig. 5. Duffing oscillator, effect of nonlinear stiffness α on condition number.

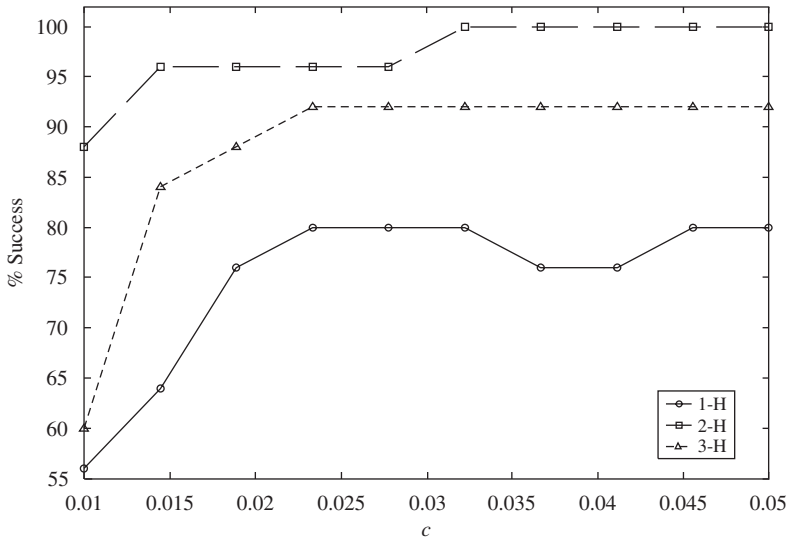

Fig. 6. Duffing oscillator: percentage success variation with damping c.

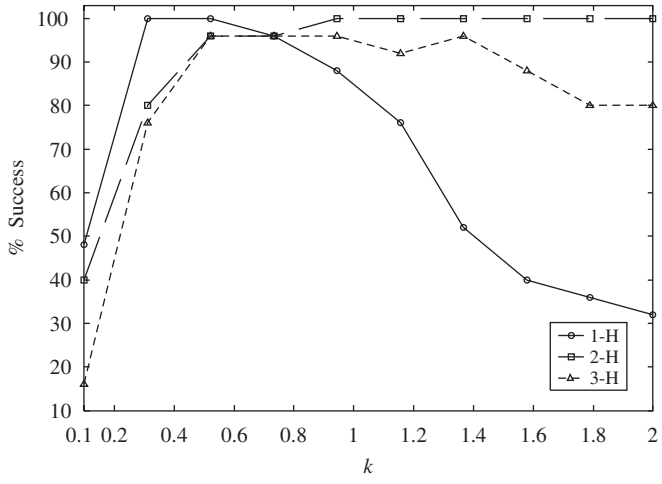

Fig. 7. Duffing oscillator: percentage success variation with linear stiffness k.

4.3. Linear system

The present method is applied to a linear system. For a parameter set as given in Table 6, the comparison is done over the range of excitations as given. The summary of the results shows that 1-H is a failure. For 1-H excitation, the first and third columns of $[G]$ matrix are linearly dependent and hence inversion will not be proper. Viewing this in HBM form, there is only one harmonic to compare whereas the number of parameters are three. Thus, the algebraic set of harmonic balance equations is under-determined. The 2-H excitation effectively gives three independent equations as the second harmonic part of the excitation is having a phase shift. This demonstrates that two harmonic inputs are quite necessary for using this identification scheme.

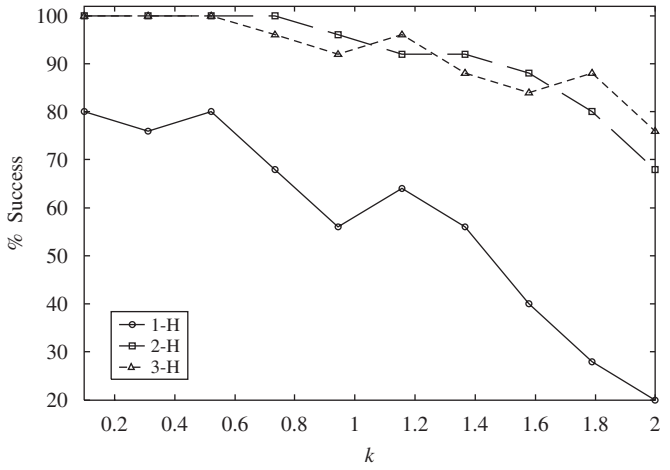

Fig. 8. Oscillator with quadratic damping. Percentage success variation with linear stiffness k.

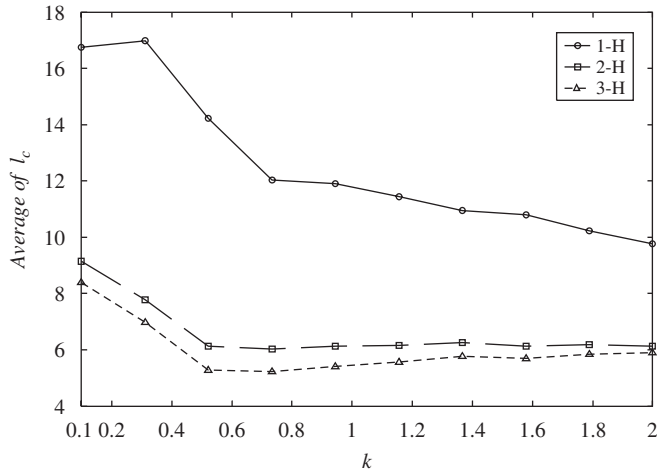

Fig. 9. Quadratic damping, effect of k on condition number.

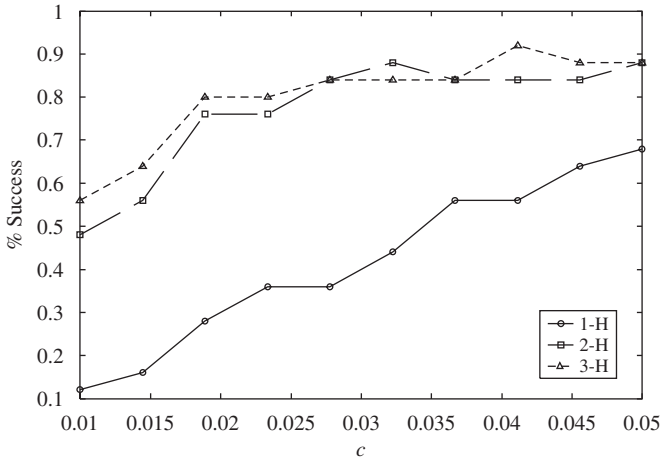

Fig. 10. Quadratic damping: percentage success variation with damping c.

Table 6
Linear system identification

$m=1$, $c=0.03$, $k=1$			
F: 0.1–2; $\eta=0.1$–0.5, number of trials $n=100$ (10×10)			
	1-H	2-H	3-H
% Success, $E_p<0.05$	10	100	100
Average of l_c	23.5119	5.4286	4.510

4.4. Multidegree of freedom (mdof) system

A three dof system shown in Fig. 11 is identified using 1-H, 2-H and 3-H excitations. The basic formulation as given in Section 2 is extended to this case. Referring to the figure, $[k_1]=\begin{bmatrix}k_{11} & k_{12} & \dots & k_{1s_1}\end{bmatrix}$, $[k_2]=\begin{bmatrix}k_{21} & k_{22} & \dots & k_{2s_2}\end{bmatrix}$ and $[k_3]=\begin{bmatrix}k_{31} & k_{32} & \dots & k_{3s_3}\end{bmatrix}$ are the coefficients of the polynomial type stiffness, and s_1, s_2 and s_3 are the respective number of polynomial terms in the nonlinear stiffness.

The damping is considered as either viscous or quadratic type. For instance, the equations of motion for the case where c_3 is quadratic damping are

$$m_1\ddot{x}_1+\sum_{i=1}^{s_1}k_{1i}x_1^i+c_1\dot{x}_1-\sum_{i=1}^{s_2}k_{2i}(x_2-x_1)^i-c_2(\dot{x}_2-\dot{x}_1)=0,$$

$$m_2\ddot{x}_2+\sum_{i=1}^{s_2}k_{2i}(x_2-x_1)^i+c_2(\dot{x}_2-\dot{x}_1)-\sum_{i=1}^{s_3}k_{3i}(x_3-x_2)^i-c_3(\dot{x}_3-\dot{x}_2)|(\dot{x}_3-\dot{x}_2)|=0,$$

$$m_3\ddot{x}_3+\sum_{i=1}^{s_3}k_{3i}(x_3-x_2)^i+c_3(\dot{x}_3-\dot{x}_2)|(\dot{x}_3-\dot{x}_2)|=f_3(t), \tag{17a–c}$$

where $f_3(t)$ is the external excitation acting on mass 3. The system of equations is numerically solved. The steady-state response, which is periodic, is taken for analysis. The FFT of the time series x_1, x_2 and x_3 is carried out. Let Ω be the fundamental frequency of the total six-dimensional orbit. The three-dimensional equivalent of Eq. (7) for Eqs. (17) will take the following form, where the algebraic details are omitted:

$$\begin{bmatrix}[G]_{11} & [G]_{12} & [0]\\ [0] & [G]_{22} & [G]_{23}\\ [0] & [0] & [G]_{33}\end{bmatrix}\begin{Bmatrix}\{r\}_1\\ \{r\}_2\\ \{r\}_3\end{Bmatrix}=\begin{Bmatrix}\{0\}\\ \{0\}\\ \{f_3\}\end{Bmatrix}. \tag{18}$$

The external force on mass m_3 is $\{f_3\}=\begin{bmatrix}f_3(1) & \cdots & f_3(N)\end{bmatrix}^{\mathrm{T}}$. The three sets of parameters are

$$\{r\}_1=\begin{bmatrix}m_1 & c_1 & k_{11} & \dots & k_{1s_1}\end{bmatrix}^{\mathrm{T}},\quad \{r\}_2=\begin{bmatrix}m_2 & c_2 & k_{21} & \cdots & k_{2s_2}\end{bmatrix}^{\mathrm{T}},$$

$$\{r\}_3=\begin{bmatrix}m_3 & c_3 & k_{31} & \dots & k_{3s_3}\end{bmatrix}^{\mathrm{T}}. \tag{19}$$

The parameters are identified in the following sequence as

$$[G]_{33}\{r\}_3=\{f_3\}\Rightarrow\{r\}_3=[G]_{33}^{+}\{f_3\},$$

$$[G]_{22}\{r\}_2+[G]_{23}\{r\}_3=\{0\}\Rightarrow\{r\}_2=-[G]_{22}^{+}[G]_{23}\{r\}_3,$$

$$[G]_{11}\{r\}_1+[G]_{12}\{r\}_2=\{0\}\Rightarrow\{r\}_1=-[G]_{11}^{+}[G]_{12}\{r\}_2. \tag{20a–c}$$

4.4.1. Numerical example

Consider a system with the parameters as given in Table 7(a). The excitation is given on the third mass. The excitation parameter range is $F_{\min}=500$, $F_{\max}=1500$, $\eta_{\min}=0.2$, $\eta_{\max}=0.8$ where $\eta_1=\Omega/\omega_{n1}$, ω_{n1} is the first undamped natural frequency of the system. The undamped natural frequencies of the system are 26.2,

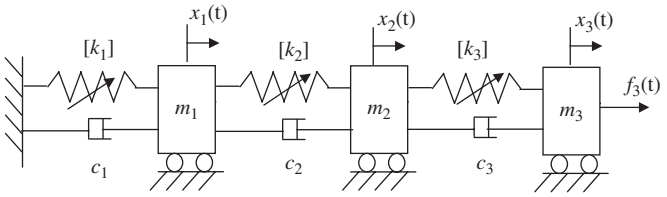

Fig. 11. A schematic of the mdof system considered for identification.

Table 7a
mdof system parameters

Mass, kg	Stiffness, N/m $\times 10^4$	Damping, N s/m $\times$ 10^3
$m_1 = 1$	$k_1 = 1$ (linear)	$c_1 = 0.04$ (quadratic)
$m_2 = 2$	$[k_2] = [0.5\ 0.1]$ (Duffing)	$c_2 = 0.03$ (viscous)
$m_3 = 2.5$	$k_3 = 2$ (linear)	$c_3 = 0.02$ (quadratic)

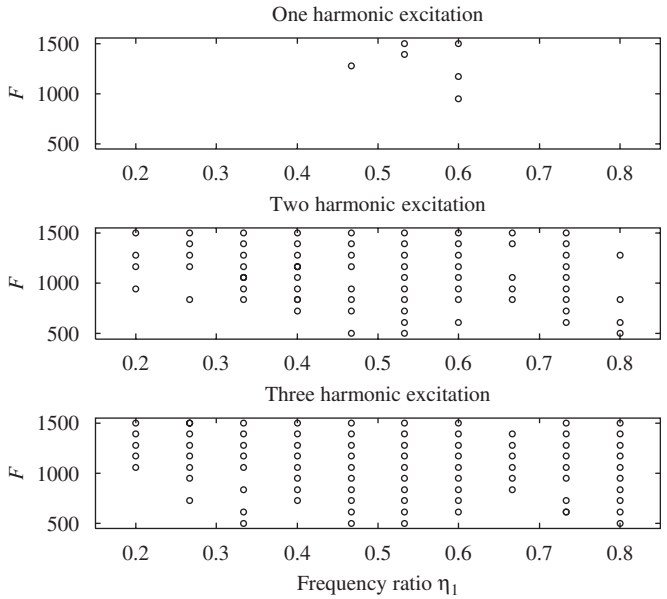

Fig. 12. mdof system: success over the excitation parameter space $F-\eta_1$, for three cases of excitation. Symbol '○' stands for $E_p \leqslant 0.05$. The blank spaces correspond to either $E_p > 0.05$ or the response being non-P1 type.

118.1 and 144.4 rad/s. Thus the excitation is below the first natural frequency. The criterion of the rms equality used in this case is the same as given in Section 3. The result of the 100 trials using a uniform grid in the above range of force and frequency is given in Fig. 12 and Table 7(b). The condition numbers associated with the matrices $[G]_{11}^{\mathrm{T}}[G]_{11}$, $[G]_{22}^{\mathrm{T}}[G]_{22}$ and $[G]_{33}^{\mathrm{T}}[G]_{33}$ are denoted by $l_{c1,}$ l_{c2} and l_{c3}, respectively. In this case, 2-H and 3-H excitations give a large improvement in results over 1-H. A reason for the improvement can again be attributed to the drop in the condition number, especially in l_{c3}.

5. Comparison studies by random generation of excitation parameter set

There is another way to obtain and present the comparative results for the various cases explained before, by using a random generation of the excitation parameters. This method is illustrated here for the Duffing oscillator (Sections 3–4) for single and multiharmonic force excitation. The excitation parameters are

Table 7b
mdof system identification results

$n = 10 \times 10 = 100$	1-H	2-H	3-H
% Success, $E_p < 0.05$	6	68	81
Average of l_{c1}	14.5914	12.7808	13.2848
Average of l_{c2}	20.1275	18.7803	19.0273
Average of l_{c3}	20.1639	16.7550	17.1822

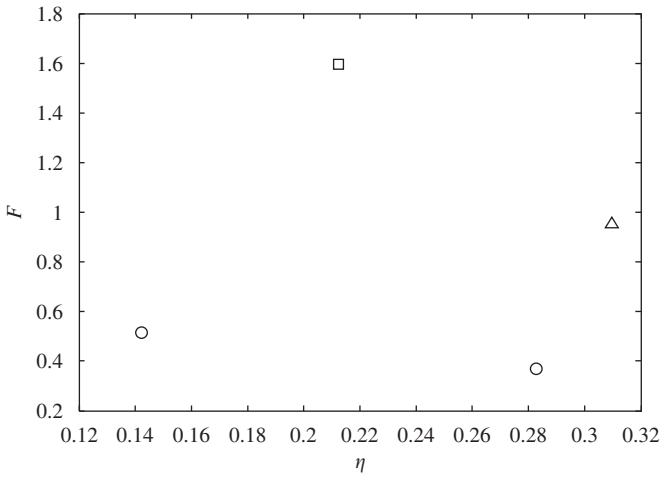

Fig. 13. Identification trials by random selection of excitation parameters. Symbols: ○—failure, Δ—first success, □—second success. At the end of second success, the total count is made. In this case, it is 4.

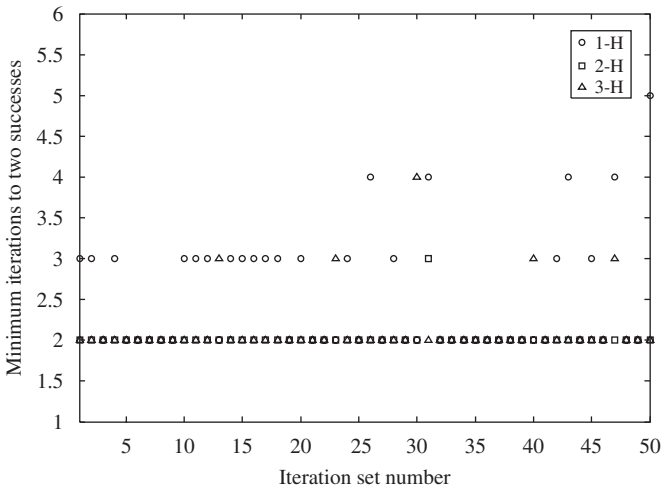

Fig. 14. Trial set as in Fig. 13 is repeated 50 times for single and multiexcitations.

generated randomly having a uniform probability distribution within a selected range of $F-\eta$. Identification is carried out for a number of trials until two results are successful ($E_p < 5\%$) and nearly match. The minimum number of trials required for two successful tests is taken as an indicator of the effectiveness of the method. The system and excitation parameters are the same as given in Table 6 with $\alpha = 0.2$. The process is illustrated

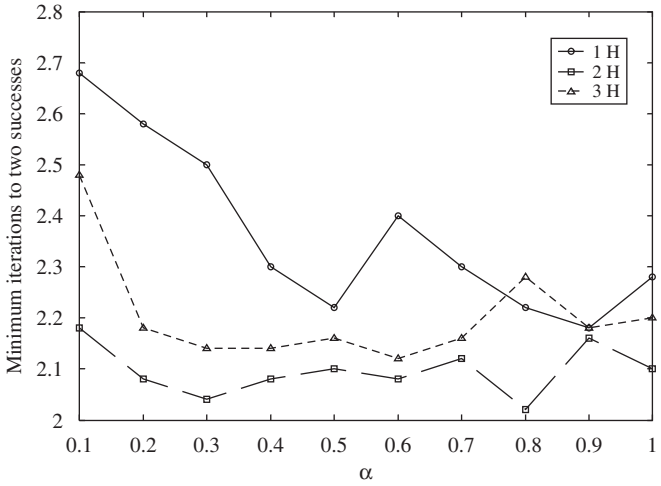

Fig. 15. The average number of trial values to success as a system parameter is varied.

in Figs. 13–14. In experimental situations, these are the kind of trials that need to be done for getting proper results. Now this experiment is repeated several times to get an average number of trials required for getting the minimum of two successes. Continuing with the earlier task of improving the excitation with multiharmonic excitation, one gets the results as shown in Fig. 14 for one, two and three harmonic excitations, with forces as given in Table 2. The average value of the minimum number of trials for two successes for the above 50 iterations are $av_1 = 2.54$, $av_2 = 2.08$ and $av_3 = 2.24$ for 1-H, 2-H and 3-H excitations, respectively. The information content of this figure is similar to that of Fig. 3. It is clear that the two-harmonic excitation is most effective in this case.

Further, it is possible to get a comparison among the three excitations while any one of the system parameters is varied. Fig. 15 shows such a comparison plot. At each of the 10 values of α, 50 iterations are done as in Fig. 14 to obtain this plot. This result is nearly matching with the results of Fig. 4. This suggests to the experimenter that the choice of multiharmonic signals is better than a single harmonic. Again, this figure may be compared with Fig. 4, as parameters used are the same.

6. Discussion and conclusions

Single harmonic excitation is found to have deficiency when used as an excitation signal for parametric system identification. To overcome this deficiency, a multiharmonic excitation is proposed. A simulation study is carried out using a hybrid frequency/time-domain method, FSIM, to investigate the success of the identification for single vs. multiharmonic excitation cases. Excitations 2-H/3-H of the form suggested is found to give improvement in the identification results considerably. The l_c associated with the multiharmonic excitation has been considerably reduced compared with the l_c of a numerically ill-posed problem with 1-H excitation. Further, a comparative study of FSIM and HBM is done and the condition for the equivalence of results in the time domain and frequency domain is established.

More studies are necessary to discern result patterns for other nonlinear systems. The choice of the excitation parameters may be done specific to each particular class of systems such as Duffing oscillator. This will involve the study of the individual nonlinear dynamics of systems that influence the numerical estimates of the parameters. Thus, the present scheme can be tailor made for any system. The usefulness of this study is not in the particular results it has generated but from the fact that it highlights the need for carrying out such an investigation for proposing guidelines for the selection of an appropriate periodic test signal for successful experimental system identification.

Appendix A. Identification: a comparison between time-domain and frequency-domain methods

In the original proposition of identification using HBM by Yasuda et al. [6], a frequency-domain method is used whereas FSIM uses a Fourier series solution to calculate a time series, which is followed by a minimization. This needs a clarification and the details are given here.

For the parametric identification, in Section 2, the form $[G]\{r\} = \{f\}$ was used. This equation is in the time domain. The columns of $[G]$ constitute the time series of $\ddot{x}(t), \dot{x}(t), x(t)$, etc. for one a time period of the fundamental excitation frequency and $\{f\}$is the time series of excitation. All these quantities are assumed to be periodic with the same fundamental period. Let the actual system response be denoted by$x'(t)$. A very small, specified truncation is done on the Fourier series of$x'(t)$ as mentioned in Section 2.3. The time series of the truncated Fourier series with M term harmonics is denoted as $x(t)$. All quantities in $[G]$ are calculated based on $x(t)$. Eq. (7) can be viewed in an alternate form in the frequency domain. For this, obtain the Fourier series of all the columns of $[G]$. For columns associated with nonlinear terms, carry out an N point FFT of the time series and obtain the Fourier coefficients. Moreover, $f(t)$ is already known in the Fourier form. Thus, the Fourier form of an equation where $f(t) = F_0 + F_{\cos}(\Omega t)$ can be written as

$$\begin{bmatrix} a_{10} & a_{20} & \cdots & a_{n_p 0} \\ a_{11} & a_{21} & \cdots & a_{n_p 1} \\ b_{11} & b_{21} & \cdots & b_{n_p 1} \\ \vdots & \vdots & \vdots & \vdots \\ a_{1M_x} & a_{2M_x} & \cdots & a_{n_p M_x} \\ b_{1M_x} & b_{2M_x} & \cdots & b_{n_p M_x} \end{bmatrix} \begin{Bmatrix} r_1 \\ r_2 \\ \vdots \\ r_{n_p} \end{Bmatrix} = \begin{Bmatrix} F_0 \\ F \\ 0 \\ \vdots \\ 0 \\ 0 \end{Bmatrix}, \tag{A.1}$$

where $M_x = (N/2-1)$. Note that $M_x > M$ due to the presence of nonlinear terms. For the columns corresponding to linear terms, the terms from $M+1$ to M_x is kept equal to zero. The parameters can be determined using a pseudo-inversion. It can be shown numerically that the result of identification is same in the two cases provided energy equivalence is satisfied. From Parseval's theorem [13], we have $\int_{-\infty}^{\infty} |x(t)|^2 \, \mathrm{d}t = \frac{1}{2\pi}\int_{-\infty}^{\infty} |X(\omega)|^2 \, \mathrm{d}\omega$, where $X(\omega)$ is the Fourier transform of $x(t)$.

The Parseval's equality for a real Fourier series takes the form

$$\frac{1}{T}\int_0^T |x'(t)|^2 \, \mathrm{d}t = a_0^2 + \frac{1}{2}\sum_{j=1}^{\infty}(a_j^2 + b_j^2).$$

For a truncated Fourier series with M harmonics, the above equality has the form

$$\frac{1}{T}\int_0^T |x(t)|^2 \, \mathrm{d}t = a_0^2 + \frac{1}{2}\sum_{j=1}^{M}(a_j^2 + b_j^2), \tag{A.2}$$

where $x(t) = a_0 + \sum_{j=1}^{M}(a_j \cos j\Omega t + b_j \sin j\Omega t)$. It follows that for preserving energy equivalence in the time domain and the frequency domain, Eq. (A.1) has to be modified as

$$\begin{bmatrix} \sqrt{2}a_{10} & \sqrt{2}a_{20} & \ldots & \sqrt{2}a_{n_p 0} \\ a_{11} & a_{21} & \ldots & a_{n_p 1} \\ b_{11} & b_{21} & \ldots & b_{n_p 1} \\ \vdots & \vdots & \vdots & \vdots \\ \vdots & \vdots & \vdots & \vdots \\ a_{1M_x} & a_{2M_x} & \ldots & a_{n_p M_x} \\ b_{1M_x} & b_{2M_x} & \ldots & b_{n_p M_x} \end{bmatrix} \begin{Bmatrix} r_1 \\ r_2 \\ \vdots \\ \vdots \\ r_{n_p} \end{Bmatrix} = \begin{Bmatrix} \sqrt{2}F_0 \\ F \\ 0 \\ \vdots \\ \vdots \\ 0 \\ 0 \end{Bmatrix}. \tag{A.3}$$

Eq. (A.3) can be written as

$$[\bar{G}]\{r\} = \{\bar{f}\}, \tag{A.4}$$

where the jth column of $[\bar{G}]$ is constituted from an ordered set of Fourier series coefficients obtained from the jth column of $[G]$, and is given by

$$\bar{G}(j) = \begin{bmatrix} \sqrt{2}a_{j0} & a_{j1} & b_{j1} & \dots & a_{jM_x} & b_{jM_x} \end{bmatrix}^{\mathrm{T}}.$$

Eq. (A.4) represents the balance of harmonics. The parameters are obtained as

$$\{r\}_i = [\bar{G}]^{+}\{\bar{f}\}. \tag{A.5}$$

Thus, Eq. (A.3) is to be used instead of Eq. (A.1) in an identification process using HBM.

Theorem. *The identification results are equal for the time-domain formulation and the frequency-domain formulation if the energy equivalence is satisfied.i.e. If* $\{r\}_1 = [G]^{+}\{f\}$ *and* $\{r\}_2 = [\bar{G}]^{+}\{\bar{f}\}$ *then* $\{r\}_1 = \{r\}_2$.

Proof. The proof is a direct consequence of Plancherel's theorem which states that the inner product of two signals $x_1(t)$ and $x_2(t)$ in time domain is equal to the inner product of their expansion coefficients α and β with respect to an orthonormal basis $\{e\}$:

$$\text{If } x_1(t) = \sum_{i=1}^{M_x} \alpha_i e_i;\ x_2(t) = \sum_{i=1}^{M_x} \beta_i e_i \quad \text{then } \langle x_1, x_2 \rangle = \langle \alpha, \bar{\beta} \rangle. \tag{A.6}$$

Adapting this theorem to the real Fourier series and using the present notations, we have

$$x_1(t) = a_{10} + \sum_{j=1}^{M_x} (a_{1j}\cos j\Omega t + b_{1j}\sin j\Omega t);\ x_2(t) = a_{20} + \sum_{j=1}^{M_x} (a_{2j}\cos j\Omega t + b_{2j}\sin j\Omega t). \tag{A.7}$$

Using orthogonality relations in the trigonometric series, it can be shown that for a period T,

$$\int_T x_1(t)x_2(t)\,\mathrm{d}t = T\left(a_{10}a_{20} + \frac{1}{2}\sum_{j=1}^{M_x}(a_{1j}a_{2j} + b_{1j}b_{2j})\right). \tag{A.8}$$

The discrete time version of the above equation is

$$\sum_{j=1}^{N} x_1[j]x_2[j] = \frac{N}{2}\begin{bmatrix} \sqrt{2}a_{10} & a_{11} & b_{11} & \dots & a_{1M_x} & b_{1M_x} \end{bmatrix}\begin{bmatrix} \sqrt{2}a_{20} & a_{21} & b_{21} & \dots & a_{2M_x} & b_{2M_x} \end{bmatrix}^{\mathrm{T}}. \tag{A.9}$$

We have, $D_{\mathrm{ij}} = \sum_{k=1}^{N} G_{ik}G_{kj}$ and it follows that

$$\bar{D}_{ij} = \sum_{k=0}^{2M_x} \bar{G}_{ik}\bar{G}_{kj} = 2a_{i0}a_{0j} + \sum_{k=1}^{M_x}(a_{ik}a_{kj} + b_{ik}b_{kj}). \tag{A.10}$$

$$D_{ij} = \frac{N}{2}\bar{D}_{\mathrm{ij}} \quad \text{and} \quad [D] = \frac{N}{2}[\bar{D}]. \tag{A.11}$$

Similarly, using the notations $\{h\} = [G]^{\mathrm{T}}\{f\}$ and $\{\bar{h}\} = [\bar{G}]^{\mathrm{T}}\{\bar{f}\}$, we get $\{h\} = \frac{N}{2}\{\bar{h}\}$.

Thus, $\{r\}_1 = [D]^{-1}\{h\} = \frac{2}{N}[\bar{D}]^{-1}\frac{N}{2}\{\bar{h}\} = [\bar{D}]^{-1}\{\bar{h}\} = \{r\}_2$. Hence the proof. □

Thus, it follows that a minimization of the mean square error in time/frequency domain will lead to the minimization of error in the frequency/time domain. A numerical illustration of the theorem is given below. Consider a system with polynomial type nonlinearity given by the equation

$$m\ddot{x} + c\dot{x} + k_1x + k_2x^2 + k_3x^3 = F_0 + F\cos\Omega t. \tag{A.12}$$

The system and the excitation parameters are given in the first row of Table A1. The identified parameters are identical in both the time-domain method as well as the frequency-domain method for any tolerance used in the truncation of Fourier series. The parametric error and the condition number are listed in the table.

Table A1
Comparison of time-domain and frequency-domain methods

System parameters: $m = 1$, $c = 0.03$, $[k] = [1,0.1,0.2]$
Excitation parameters: $F_0 = 0.02$, $F = 0.5$, $\eta = 0.2$

ε	Time-domain method		Frequency-domain method	
	E_p	l_c	E_p	l_c
10^{-2}	0.40	12.23	0.40	12.23
10^{-4}	0.13	12.29	0.13	12.29
10^{-6}	0.0057	10.99	0.0057	10.99

The first row in Eq. (A.3) is to weighted with $1/\sqrt{2}$ to get the first row of Eq. (A.1) and hence the two identification results (using Eqs. (A.1) and (A.3)) would be different if nonzero mean value is present in the solution. A mean offset in displacement can occur in nonlinear systems subjected to harmonic inputs.

A.1. Identification using HBM

The difference between HBM and FSIM is summarized in Fig. 1. HBM is a frequency-domain method in which higher-order harmonics are not considered in the final solution. It is seen that the removal of higher order harmonics of negligible values in Eq. (A.3) improves the identification results in comparison to the case where all terms are retained. However, this has to be done carefully as the removal of any row with a nonzero entry may lead to large errors, since the entire set of equations are to be satisfied simultaneously. In FSIM, these considerations are not required.

Appendix B. Error correlation studies in identification

B.1. Parametric error

In the parametric identification of systems, the aim is to obtain the actual values of the system parameters in the system model. An error in the parametric identification can be defined based on the true values of the parameters and the corresponding identified values. Let $\{r_o\}$ be the set of original parameter values and let the identified parameter set be $\{r_i\}$ and the number of parameters be n_p. A normalized parametric error can be obtained for each parameter as $p_j = (r_i(j) - r_o(j))/r_o(j)$. The parametric error in the identification can be defined as

$$E_p = \sqrt{p_j^{\mathrm{T}} p_j / n_p}. \tag{B.1}$$

Thus, E_p is a measure of the error in parametric identification. A correct identification scheme should yield a value of E_p close to zero. Though Eq. (B.1) is a simple way of defining the error, it cannot be estimated in an experiment as this is defined in terms of actual system parameters, which are unknown. If the identification is carried out using the simulated data as done in the present study, the parameters of the original and the identified system are available for error estimation and the above measure can be used to assess the correctness of the identification scheme.

B.2. RMS error between the response signals of the original and the identified system

The rms value of a signal $x(t)$ over a length of time T is $E_r = \sqrt{\frac{1}{T}\int_{t=0}^{T}[x(t)]^2\,\mathrm{d}t}$. Let $x_o(t)$ be the original signal. Using the identified parameter values, a response signal $x_i(t)$ can be generated by simulation. The original and the identified signals may be taken either from the initial transient portion of the response or from the steady-state response. For these two signals, $x_o(t)$ is taken as a reference signal and the rms error in $x_i(t)$ is defined as in Eq. (12). In the identification context, response trajectory of the system $x_o(t)$ is available. System

identification is carried out to get the parameters $\{r_i\}$. Using this identified parameters, a response trajectory $x_o(t)$ can be simulated for the same system model with identical input. Thus, E_r gives a measure of the quality of identification. This measure can be used for the experimental case also and is one of the most common practices of estimating error in the identification.

B.3. RMS error for the applied force and the force induced by the identified parameters

Let $f(t)$ be the system excitation. This force is balanced by the sum of various forces developed in the system. For example, consider a Duffing oscillator given by the equation $m\ddot{x} + c\ddot{x} + kx + \alpha x^3 = f(t)$. The system identified values may be substituted in the above equation to obtain an induced force $f_{\mathrm{i}}(t)$. Error estimated using the identified parameters, $e(t) = f_i(t) - f(t)$and the total mean square error in force over a length of time T is

$$E_f = \sqrt{\frac{1}{T}\int_0^T [e(t)]^2 \, \mathrm{d}t}. \tag{B.2}$$

B.4. Illustration example

There are instances where the rms-based error norms can give wrong results. To illustrate this point the identification of a harmonically forced Duffing oscillator is considered. Consider two tests with the specified

Table B1
Comparison of two excitations

Excitation: $F\cos(\Omega t)$, frequency ratio $\eta = (\Omega/\omega_n)$, excitation parameters: (F, η)								
System parameters	m	c	K	α	EP	E_p	E_r	E_f
	2	0.02	1	0.2				
Ident. parm., test 1	1.9963	0.0200	0.9997	0.2002	0.5, 0.3	0.0008	0.0001	0.0000
Ident. parm., test 2	2.4790	0.0204	1.0427	0.0406	0.4, 0.3	0.2084	0.0005	0.0001

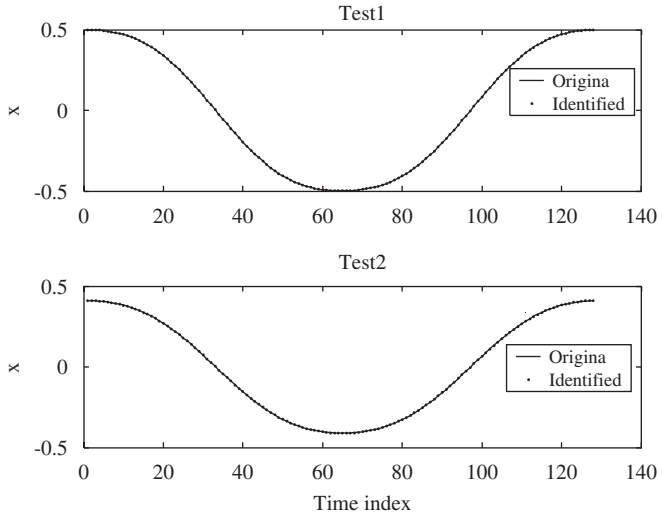

Fig. B1. Displacement response of a Duffing oscillator for two different inputs.

harmonic excitations and the results given in Table B1. The errors in the identification E_p, E_r and E_f for the two tests are given in the table. The first test gives accurate result whereas the second has a result with about 20% parametric error. However, the rms errors (E_r and E_f) in both cases are extremely small. The time series of the displacement for the original and the identified system are shown in Fig. B1. The applied force and the corresponding induced force using the identified values are compared in Fig. B2. In both these figures these are in close agreement. Thus, the low values of rms errors do not necessarily imply that the parametric error is small. Note that the E_p is not available in a real identification and the interpretation based on E_r and E_f may lead to wrong results in this case. Hence, an identification scheme should be good enough to overcome such misleading results.

B.5. Correlation between E_p, E_r and E_f

In order to obtain a relationship between various errors a qualitative study was made. A Duffing oscillator with chosen parameters was subjected to a set of harmonic excitations. In each case, the system was identified.

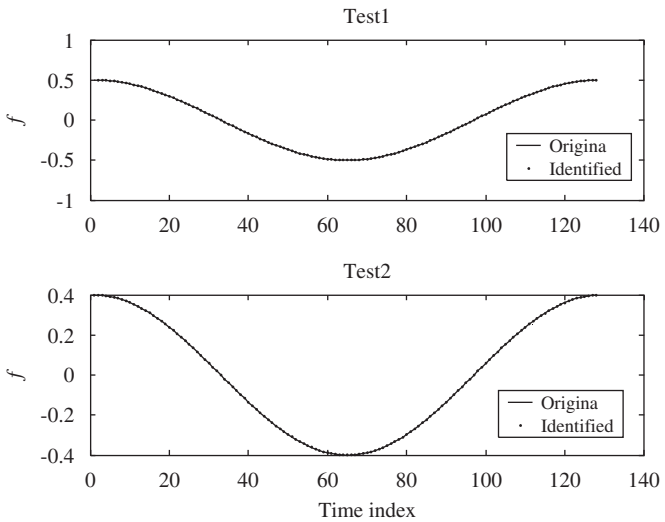

Fig. B2. Excitation force of a Duffing oscillator for two different inputs.

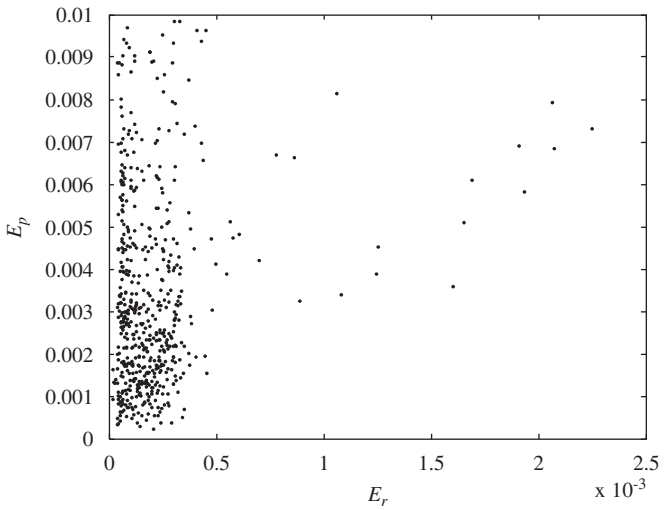

Fig. B3. E_p and E_r are not correlated.

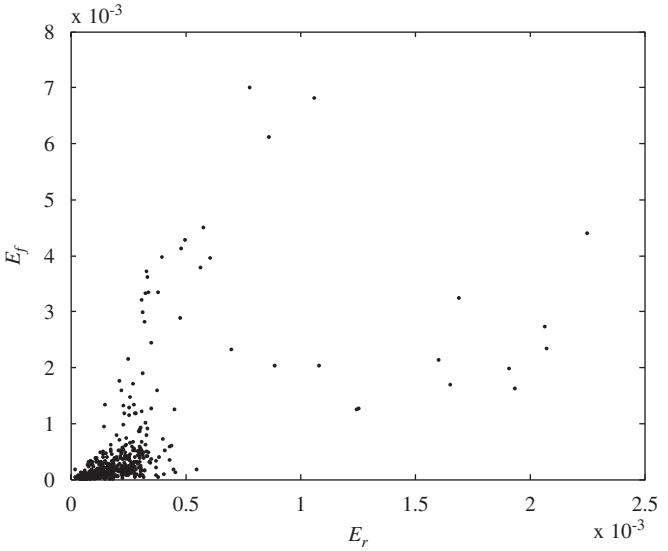

Fig. B4. E_f and E_r are correlated.

The three errors E_p, E_r and E_f were estimated. One thousand tests were conducted. The results for which $E_p<0.01$, are considered. Fig. B3 shows E_p vs. E_r and there is apparently no visible correlation between the two quantities. It is also clear that the minimum of the trajectory error will not yield a minimum of parametric error. On the other hand, Fig. B4 shows E_r vs. E_f, in which there is a conical structure close to the origin. Since there is a definite relationship between $x(t)$ and $f(t)$ through the governing differential equation, there should be a correlation between their respective errors.

References

[1] K. Worden, G.R. Tomlinson, Nonlinearity in experimental modal analysis, *Philosophical Transactions of the Royal Society of London A* 359 (2001) 113–130.
[2] S.F. Masri, T.K. Caughey, A nonparametric identification technique for nonlinear dynamic problems, *Journal of Applied Mechanics* 46 (1979) 433–447.
[3] E.F. Crawley, A.C. Aubert, Identification of nonlinear structural elements by force state mapping, *AIAA Journal* 24 (1986) 155–162.
[4] K.S. Mohammad, K. Worden, G.R. Tomlinson, Direct parameter estimation for linear and nonlinear structures, *Journal of Sound and Vibration* 152 (1992) 471–499.
[5] P. Perona, A. Porporato, L. Ridolfi, On the trajectory method for the reconstruction of differential equations from time series, *Nonlinear Dynamics* 23 (2000) 13–33.
[6] K. Yasuda, S. Kawamura, K. Watanabe, Identification of nonlinear multi-degree-of-freedom systems (presentation of an identification technique), *JSME International Journal, Series III* 31 (1988) 8–14.
[7] C.M. Yuan, B.F. Feeny, Parametric identification of chaotic systems, *Journal of Vibration and Control* 12 (1998) 405–426.
[8] M. Thothadri, R.A. Cass, F.C. Moon, R. D'Andrea, C.R. Johnson Jr., Nonlinear system identification of multi-degree-of-freedom systems, *Nonlinear Dynamics* 32 (2003) 307–322.
[9] T.A. Doughty, P. Davies, A.K. Bajaj, A comparison of three techniques using steady state data to identify non-linear modal behavior of an externally excited cantilever beam, *Journal of Sound and Vibration* 249 (2002) 785–813.
[10] M.D. Narayanan, S. Narayanan, C. Padmanabhan, Parametric identification of a nonlinear system using multi-harmonic excitation, *Proceedings VETOMAC-3 & ACSIM-2004 Conference*, Vol. 2, New Delhi, India, December 6–9, 2004, pp. 706–714.
[11] A. Ushida, L.O. Chua, Frequency-domain analysis of nonlinear circuits driven by multi-tone signals, *IEEE Transactions on Circuits and Systems* CAS-31 (1984) 766–778.
[12] V. Borich, J. East, G. Haddad, An efficient Fourier transform algorithm for multitone harmonic balance, *IEEE Transactions on Microwave Theory and Techniques* 47 (1999) 182–188.
[13] I.S. Sokolnikoff, R.M. Redheffer, *Mathematics of Physics and Modern Engineering*, McGraw-Hill, New York, 1984.